

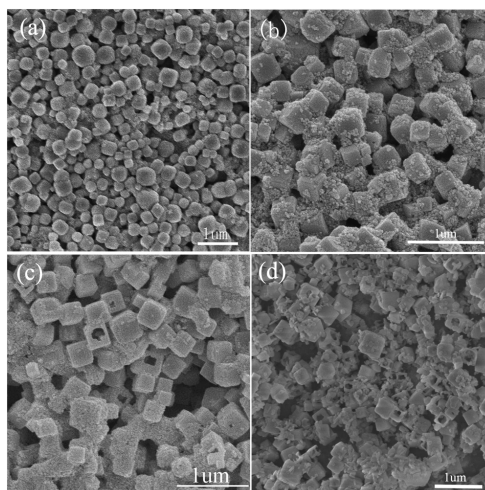
# Electronic Supplementary Information

## Synthesis of $\text{Co}_2\text{SnO}_4$ hollow cubes encapsulated in graphene as high capacity anode materials for Lithium-Ion Batteries

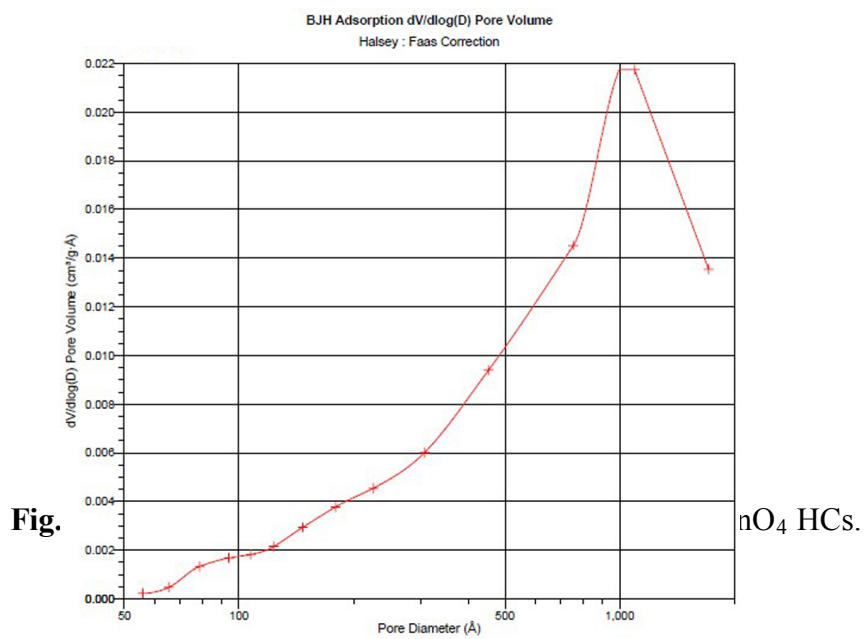
Jingjing Zhang<sup>a</sup>, Jianwen Liang<sup>a</sup>, Yongchun Zhu<sup>a,\*,\*</sup>, Denghu Wei<sup>a</sup>, Long Fan<sup>a</sup> and  
Yitai Qian<sup>a, b, \*</sup>

<sup>a</sup> Hefei National Laboratory for Physical Science at Microscale and Department of Chemistry, University of Science and Technology of China, Hefei, 230026, P.R. China. Tel: +86-551-63601589; E-mail: ychzhu@ustc.edu.cn

<sup>b</sup> School of Chemistry and Chemical Engineering, Shandong University, Jinan, 250100, PR China. Tel: +86-551-63607234; E-mail: ytqian@ustc.edu.cn

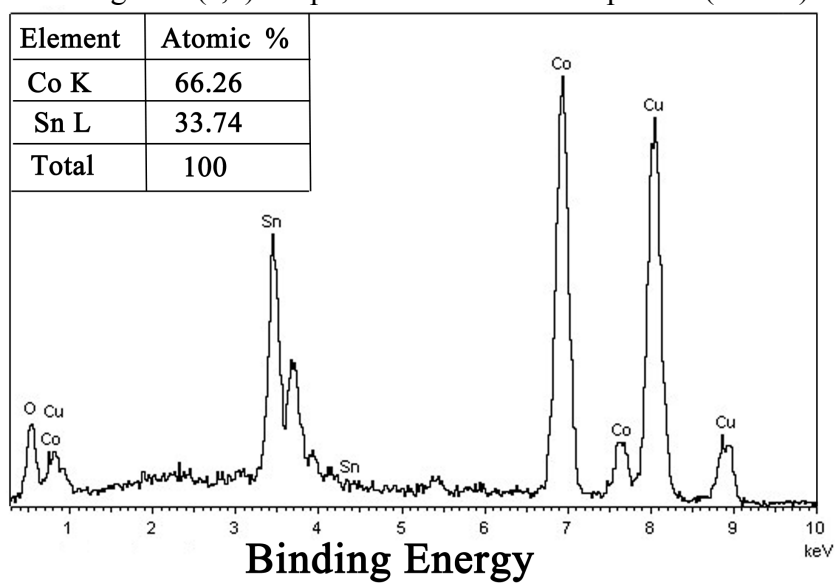


**Fig. S1.** SEM images of a series of temperature-dependent experiments of precursor (a) prepared at room temperature, (b) at 100 °C, (c) at 120 °C and (d) 140 °C.

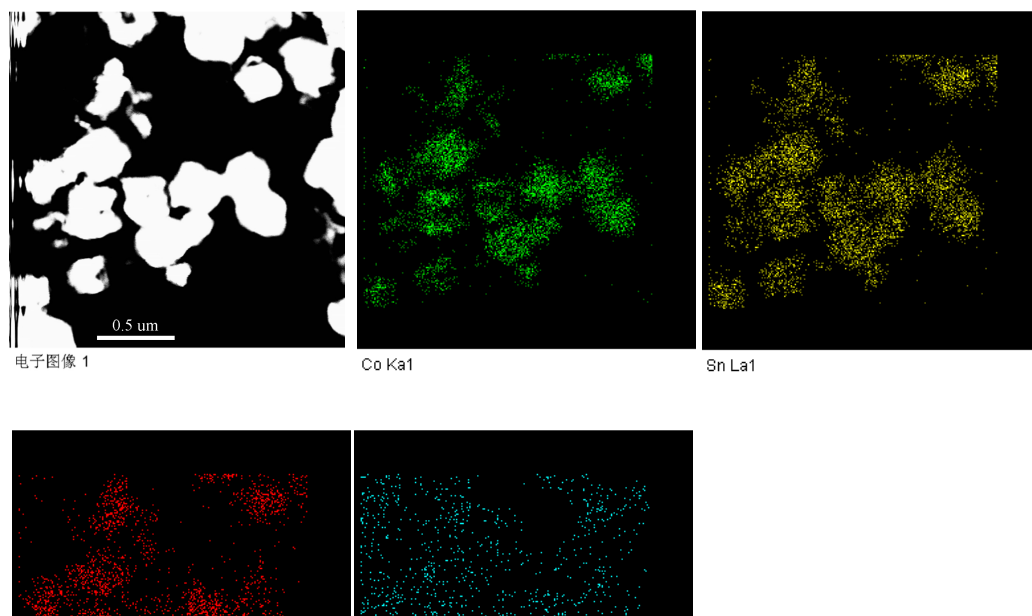


**Fig. S3.** BJH porous distribution of  $\text{Co}_2\text{SnO}_4$  HCs ( $V$  = differential pore volume,  $D$  = pore size)

**Fig. S4.** SEM images of (a,b) the precursor and its TEM pattern (inset b) and (c,d)



**Fig. S5.** Typical EDX spectrums of  $\text{Co}_2\text{SnO}_4$  HCs.



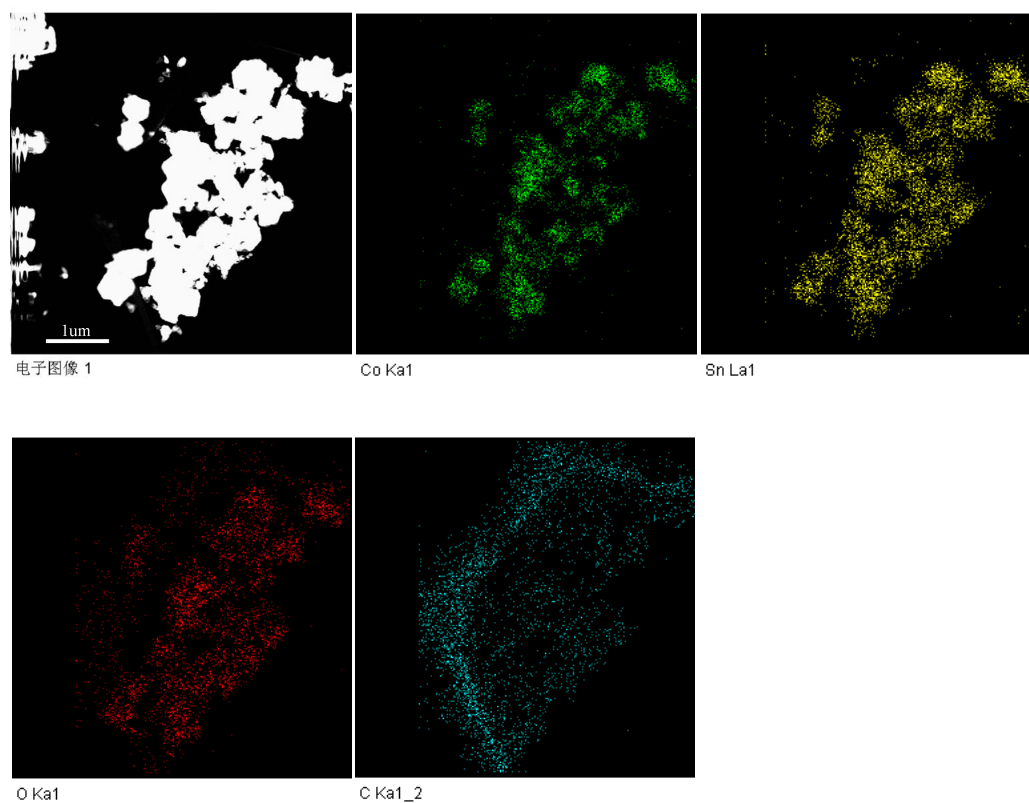


**Fig. S6.** TEM image and corresponding oxygen, cobalt, tin, and carbon elemental mapping of  $\text{Co}_2\text{SnO}_4$  HCs@GO.

**Fig. S7.** Typical XRD patterns of  $\text{Co}_2\text{SnO}_4$  HCs@rGO.

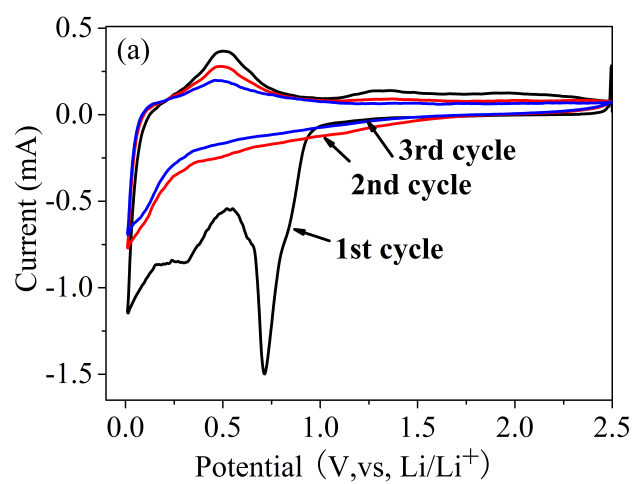


**Fig. S8.** Cyclic voltammograms of  $\text{Co}_2\text{SnO}_4$  NCs at a scanning rate of  $0.1 \text{ mVs}^{-1}$ .

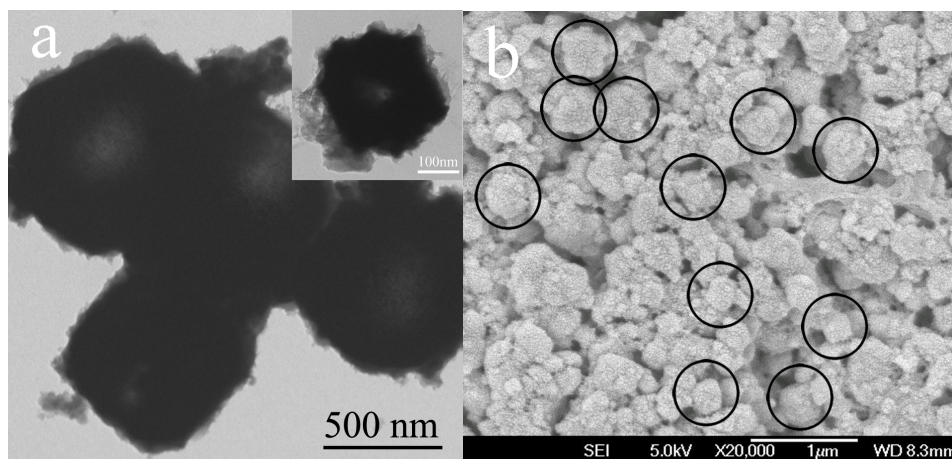


**Figure S9.** (a) TEM (high-magnification TEM image inset) and (b) FESEM images of  $\text{Co}_2\text{SnO}_4$  HCs@GO after cycling for 100cycles. In the FESEM image, the hollow cubes are marked with black circle.

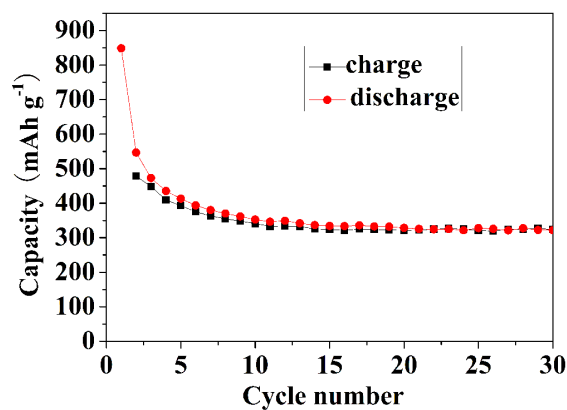


**Fig. S10.** Charge/discharge profiles of the graphite.

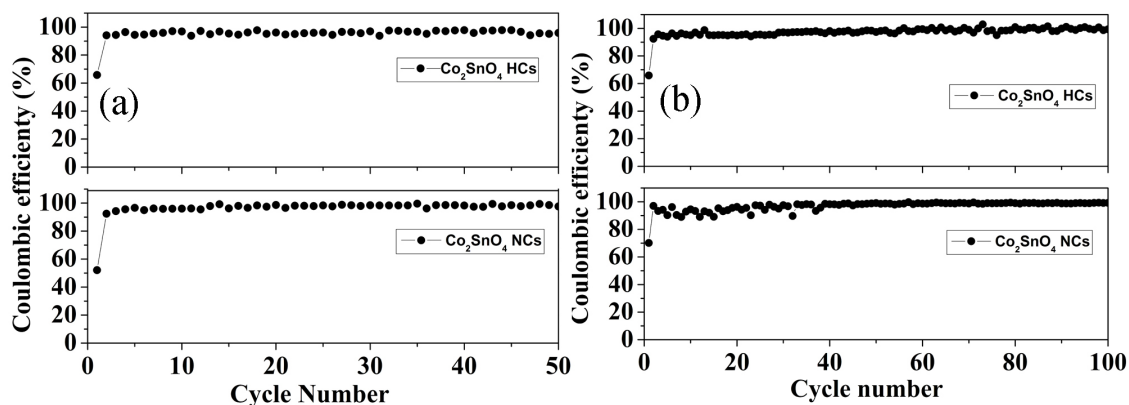


**Fig. S11.** Coulombic efficiency of (a) cycle performance at a current density of  $100 \text{ mA g}^{-1}$  between 0.01 and 2.5 V and (b) Rate capability at various current densities between 0.01 and 2.5 V for  $\text{Co}_2\text{SnO}_4$  NCs and  $\text{Co}_2\text{SnO}_4$  HCs.

For  $\text{Co}_2\text{SnO}_4$  NCs and  $\text{Co}_2\text{SnO}_4$  HCs, the coulombic efficiency maintains

consistently at ~97% up to 100 cycles (shown in Fig. S11a) and also keeps at ~97% following the rising rates (in Fig. S11b).

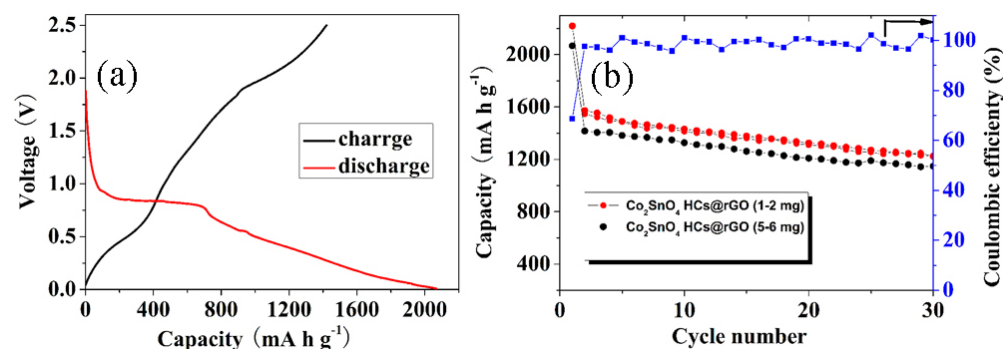


**Fig. S12.** (a) The initial discharge-charge curves for  $\text{Co}_2\text{SnO}_4$  HCs@rGO (5-6 mg) at a current density of  $100 \text{ mA g}^{-1}$  between 0.01 and 2.5 V, (b) cycle performance at a current density of  $100 \text{ mA g}^{-1}$  between 0.01 and 2.5 V, and the coulombic efficiency of the  $\text{Co}_2\text{SnO}_4$  HCs@rGO (5-6 mg).

Table 1 comparison between  $\text{Co}_2\text{SnO}_4$  hollow cubes/graphene composite ( $\text{Co}_2\text{SnO}_4$  HCs@rGO) (this work) and the reported  $\text{Co}_2\text{SnO}_4$  compounds.

Material	Reversible capacity ( $\text{mAh g}^{-1}$ )	Percentage of theoretical capacity	current density ( $\text{mA g}^{-1}$ )	Ref.
$\text{Co}_2\text{SnO}_4$ HCs@rGO	1016.2/100cycles	91.9%	100	this work
$\text{Co}_2\text{SnO}_4$ HCs	410/100cycles	37.1%	100	this work
$\text{Co}_2\text{SnO}_4$ NCs	179/100cycles	16.2%	100	this work

---

solid $\text{Co}_2\text{SnO}_4$	490/2cycles	44.3%	50	6
bulk $\text{Co}_2\text{SnO}_4$	112.8/50cycles	11%	30	8
$\text{Co}_2\text{SnO}_4$ nanocrystals	555.9/50cycles	50.3%	30	8
$\text{Co}_2\text{SnO}_4$ @C core-shell nanostructures	474/75cycles	42.8%	100	18
$\text{Co}_2\text{SnO}_4$ nanoparticles@ multiwalled carbon nanotubes	898.8/50cycles	81.3%	50	19